Reviewed Preprint
v1 • February 14, 2025
Not revised

Reviewed Preprint
v2 • May 15, 2026
Revised by authors

Genome Restructuring around Innate Immune Genes in Monocytes in Alcohol-associated Hepatitis

Adam Kim[1] ✉, **Megan R McMullen**[2], **Annette Bellar**[2], **David Streem**[3], **Jaividhya Dasarathy**[4], **Nicole Welch**[2,5,6], **Srinivasan Dasarathy**[2,5,6]

[1]Department of Medicine, University of Connecticut Health Center, Farmington, United States • [2]Northern Ohio Alcohol Center, Department of Inflammation and Immunity, Cleveland Clinic, Cleveland, United States • [3]Lutheran Hospital, Cleveland Clinic, Cleveland, United States • [4]Department of Family Medicine, MetroHealth, Cleveland, United States • [5]Department of Gastroenterology and Hepatology, Cleveland Clinic, Cleveland, United States • [6]Department of Molecular Medicine, Case Western Reserve University, Cleveland, United States

✉ **For correspondence:** adkim@uchc.edu

Competing interests: No competing interests declared

Funding: See page 15

Reviewing editor: Satyajit Rath, National Institute of Immunology, India

eLife Assessment

This potentially **useful** manuscript addresses the 3D chromatin architecture in monocytes from a few patients with alcohol-associated hepatitis and its relationship to enhanced transcription of innate immune genes. While the concept and methodological approach are interesting in principle, the evidence is **incomplete** as a result of insufficient sample sizes as well as other substantive analytical concerns.

https://doi.org/10.7554/eLife.102626.2.sa2

Abstract

Many inflammatory genes in the immune system are clustered in the genome. The 3D genome architecture of these clustered genes likely plays a critical role in their regulation and alterations to this structure may contribute to diseases where inflammation is poorly controlled. Alcohol-associated hepatitis (AH) is a severe inflammatory disease that contributes significantly to morbidity in alcohol associated liver disease. Monocytes in AH are hyper-responsive to inflammatory stimuli and contribute significantly to inflammation. We performed high throughput chromatin conformation capture (Hi-C) technology on monocytes isolated from 4 AH patients and 4 healthy controls to better understand how genome structure is altered in AH. Most chromosomes from AH and healthy controls were significantly dissimilar from each other. Comparing AH to HC, many regions of the genome contained significant changes in contact frequency. While there were alterations throughout the genome, there were a number of hotspots containing a higher density of changes in structure. A few of these hotspots contained genes involved in innate immunity including the NK-gene receptor complex and the CXC-chemokines. Finally, we compare these results to scRNA-seq data from patients with AH challenged with LPS to predict how chromatin conformation impacts transcription of clustered immune genes. Together, these results reveal changes in the chromatin structure of monocytes from AH patients that perturb expression of highly clustered proinflammatory genes.

Introduction

The three-dimensional (3D) architecture of chromatin in the nucleus is highly organized and contributes to the regulation of gene expression and cellular differentiation. Within the nucleus, each chromosome forms compartments that are distinct and separate from each other, called chromosome territories[1]. Within chromosome territories, the 3D architecture forms many distinct local features, like loops and topologically associating domains (TADs), as well as long-range

interactions between enhancers, insulators, and promoters[2]. Cohesin and CCCTC-binding factor (CTCF) determine the structure and boundaries of TADs and these structural elements are conserved in many different cell types and species[3,4]. Loss of these proteins in most cell types disrupts TAD structure and chromatin loops although surprisingly gene expression is mostly unchanged[5–7]. But in myeloid cells, loss of CTCF greatly disrupts expression of innate immune genes after acute inflammatory stimuli, suggesting local chromatin structure has a significant role in certain context specific gene expression responses[8,9].

While transcription factors, like nuclear factor-kappa B (NF-κB) and interferon-regulatory factors (IRF), bind and activate specific regulatory elements in the genome[10], the 3D genome architecture, via TADs and chromatin loops, bring these elements into close proximity, and increase associations between enhancers and promoters of genes in similar activation states[11,12]. In certain contexts, transcription factor activation can then alter the 3D genomic landscape by increasing chromatin accessibility and contact frequency of certain regions. For example, in response to type 1 and type 2 interferons, loci in the genome containing families of interferon stimulated genes, increase chromatin contacts[13].

While the 3D architecture plays a major role in cellular differentiation and gene regulation, less is known about how chromatin structure changes in disease[11,14]. A recent study, which performed high-throughput chromatin conformation capture technology (Hi-C) on primary monocytes from two patients with systemic lupus erythematosus (SLE) and two age- and sex-matched healthy controls, found few changes in chromatin structure between healthy and disease individuals[15]. This would suggest that Hi-C might not be a useful tool for predicting how monocytes transform in disease, and how genome architecture influences gene expression in primary cells. On the other hand, a few studies have found many differences in chromatin structure between primary monocytes and THP-1 cells, a monocytic cell line[15–17]. While these data suggest that 3D genome architecture may be a conserved feature of cellular differentiation and not a significant contributor to disease, more studies have to be conducted in different disease contexts to see how chromatin structure can influence monocyte gene expression. One limitation of the previous studies is that, due to the cost of these experiments, the sample size tends to be low, 1-2 patient samples, and data is often combined to increase resolution. As a result, statistical testing and disease specific comparisons have not been measured in most previous studies.

Alcohol-associated Hepatitis (AH) is a severe inflammatory disease characterized by extremely pro-inflammatory immune cells which infiltrate and damage the liver[18,19]. Monocytes in AH express significantly more pro-inflammatory genes in response to innate immune stimuli[20–22]. Many innate immune genes are clustered in the genome, like the CXC-chemokine cluster on Chromosome 4, the CC-chemokine cluster on Chromosome 17, and the NK-gene receptor complex on Chromosome 12, all of which have been implicated in AH. Single cell analysis revealed that these genes have highly coordinated expression patterns, suggesting the proximity of these genes influences their expression patterns[20].

Here, we present the 3D genome architecture of primary monocytes isolated from four patients with severe AH, and four age-matched healthy controls using Hi-C technology. We hypothesized that hypersensitivity to bacterial lipopolysaccharides (LPS) and heightened pro-inflammatory responses in AH might be due to a significantly perturbed 3D genome architecture. Our results show that there are extensive changes in chromatin structure throughout the genome in AH. While changes in contact frequency occurred throughout every chromosome, there were a number of hotspots with a high density of changes, and in many cases, hotspots contained important families of genes involved in immunity and have been implicated in AH. Ultimately, these results suggest the 3D genome structure is significantly altered in AH, and these changes contribute to perturbed gene expression patterns, specifically pro-inflammatory genes.

Results

Hi-C reveals the 3D genome architecture of hyper-inflammatory monocytes from AH patients

To investigate changes in 3D genome architecture, we performed Hi-C on primary monocytes isolated from four AH patients (all males) and 4 age-matched healthy controls (3 males and 1 female, Table 1, Supplemental Table 1). Cryo-preserved PBMCs were thawed and CD14+ and CD16+ monocytes were isolated by negative selection. Hi-C was then performed using the Arima kit, and all 8 libraries were sequenced to an average depth of about 570 million reads per sample (Supplemental Table 2). Using Juicer, the reads were aligned to the genome and chromatin conformation was determined at a resolution of 100kb. As expected, most of the chromatin interactions observed were local and intra-chromosomal (Figure 1, Supplemental Figure 1, Supplemental Table 2). As a result, we focused on intra-chromosomal analyses and not inter-chromosomal interactions.

Using HiCRep[23], we measured the correlation coefficient of the chromatin interactions for each chromosome between every sample to assess in an unbiased manner how much variation there is in genome architecture between different patients. For most comparisons, the correlation coefficient between all individuals was very high (>90%), indicative of the high conservation of 3D genome architecture in monocytes regardless of disease status. But for most chromosomes, higher correlations were observed between healthy controls or between AH samples, and not between the two groups (Figure 2), indicative of a change in genome architecture caused by disease. Notable exceptions include chromosomes 4, 11, 16, 19 and the X chromosome. For the X chromosome, one female healthy control sample (HC2) differed significantly from the 7 males, and the 3 HC males were more similar to each other than the 4 AH patients (Supplemental Figure 2). Chromosomes 4, 11, and 19 mostly showed higher similarity by disease, except the female healthy control was more similar to the AH patients. Chromosome 16 did not segregate by disease. These data indicate that while much of the 3D genome architecture of monocytes does not change with disease, there likely exist chromosome specific regions that differ significantly.

Differences in 3D Architecture occur throughout all chromosomes in AH

Hi-C data reveal regions of the genome in close proximity via the contact frequency between two loci. We can measure disease-specific changes in 3D genome architecture by measuring statistically significant differences in these frequencies. Using multiHiCcompare[24], we measured the contact frequency between every pair of 100kb genome windows (region-region pairs) and calculated statistically significant changes between HC and AH. We observed significant change in contact frequency throughout the entire length of each chromosome (Figure 3). To ensure the method was reliable, we randomized the samples 5 times prior to statistical testing and observed almost no significant changes between regions in any of the tests (Supplemental Table 3).

For most chromosomes, the changes in contact frequency caused by disease occurred in region-region pairs that are adjacent to each other, which corresponds to the fact that most Hi-C interactions are between local genomic regions (Supplemental Figure 3)[25,26]. For example, interaction data from Chromosome 2 is primarily between adjacent regions and diminishes by distance, and similarly changes in contact frequency caused by disease are also mostly local (Supplemental Figure 4). Chromosome 1 is an exception because it can be separated into 3 major megadomains, and changes in genome structure in chromosome 1 were restricted to these regions, with almost nothing differing between each megadomain (Supplemental Figure 5). Some chromosomes did have long-distance structural changes between chromosome arms, including chromosomes 11, 12, 14, 16, 17, 19, and 20. The telomeric regions of Chromosome 14 had extensive increases in contact frequency with the body of the chromosome in AH. The telomeres of Chromosome 14 contain the T-cell receptor alpha (TRA) locus on one arm and the immunoglobulin heavy chain (IGH) locus on the other.

Table 1. **Summary of Clinical data for patient samples used for Hi-C**

	Healthy Control Lean, n=4	Alcohol-associated Hepatitis Lean, n=4
Age (years)	45 (31-57)	46 (25-62)
Sex	3M/1F	4M
AST (U/L)	-	115 (30-241)
ALT (U/L)	-	44 (21-99)
Serum Albumin (g/dL)	-	3.1 (3.0-3.3)
Serum Creatinine (mg/dL)	-	1.81 (1.04-3.50)
Serum Bilirubin (mg/dL)	-	21.5 (1.9-30.9)
HBA1c	-	9.1 (7.2-10.5)
MELD Score	-	26 (14-35)

Figure 1. **Hi-C data reveals regions of the genome in close proximity**

Juicebox plot showing the contact frequency map (100kb resolution) for the entire genome with each chromosome laid end to end (X and Y chromosomes at the bottom right). Each red dot consists of two regions of the genome associated with each other. Top right: HC patient monocytes. Bottom Left: AH patient monocytes

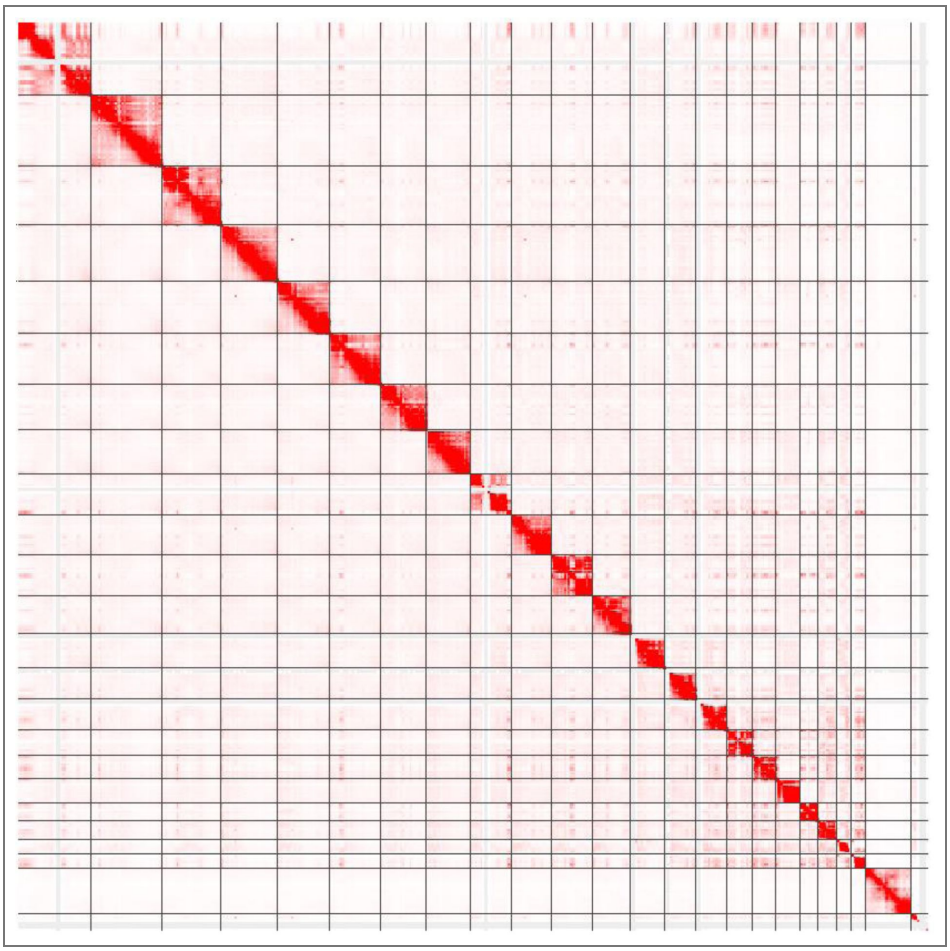

Figure 2. **Correlation reveals differences between AH and HC**

Hierarchically clustered heatmaps of correlation coefficients of the Hi-C data for each chromosome. For each heatmap, darker colors refer to higher correlation coefficients.

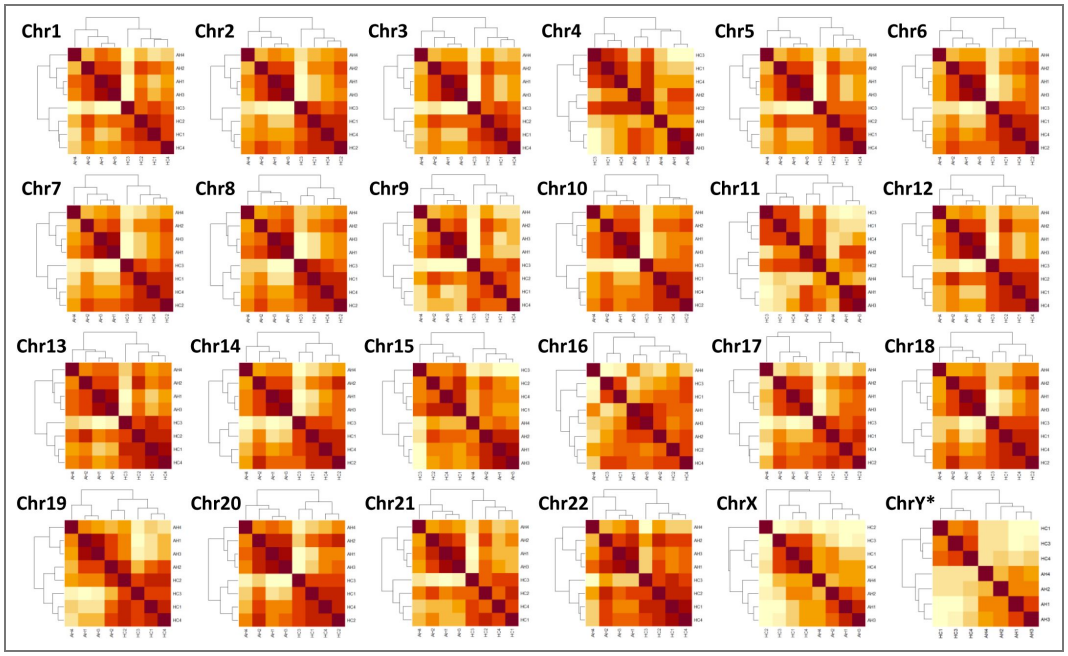

Figure 3. **Changes in Contact Frequency in Disease are Local and Long-Range**

Plots showing regions with significant changes in contact frequency in AH. Each dot indicates two regions of the genome that either increased (Blue) or decreased (Red) contact frequency in AH. X- and Y-axes are position along the chromosome

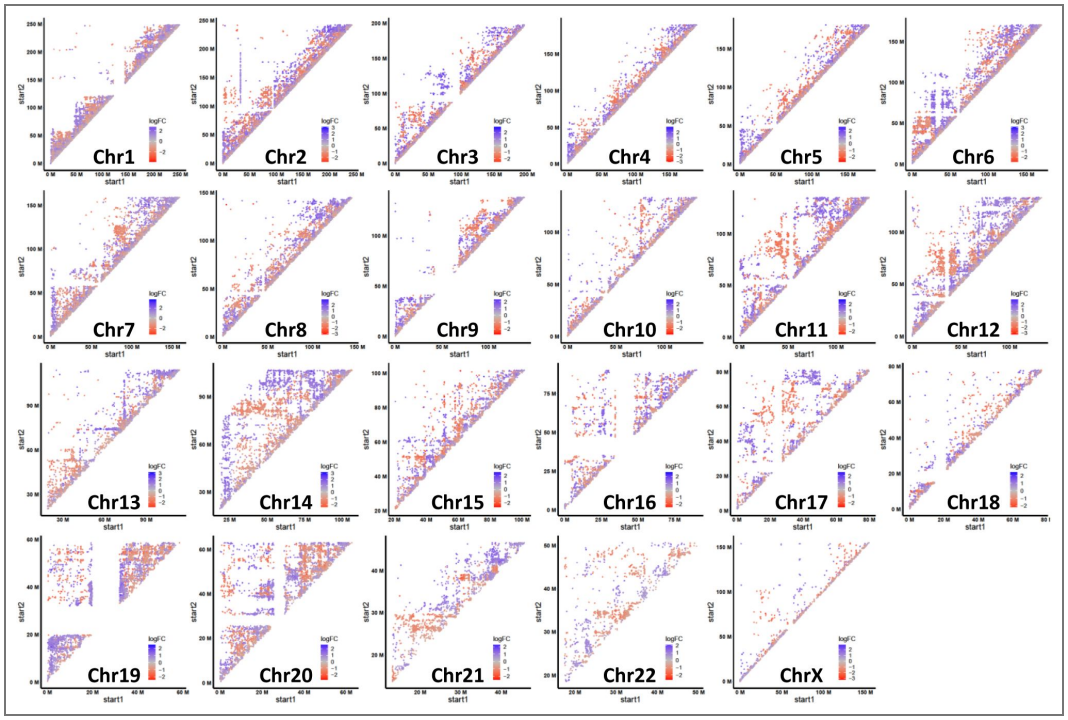

Numerous Hotspots with significant structural change in AH contain genes important for innate immunity

While there were differences in contact frequency throughout the genome in AH, there were a number of notable "hotspots" that contained a high density of the most significantly altered regions (Figure 4A). To identify these hotspots, we focused only on regions of the genome with exceptionally high statistically significant changes in contact frequency (padj<0.0000001). From this list of we identified 22 "hotspots" regions of the genome with a high frequency of these changes caused by disease (Table 2, Supplemental Table 4). The size of these hotspots varied significantly from 21MB down to less than 1MB. For most hotspots, the differences in contact frequency occurred entirely within the region. Many of the hotspots entirely increased or decreased contact frequency in AH while some contained separate areas that increased or decreased, further indicative of a localized rearrangement in genome structure, with some areas moving closer and others moving further away in disease.

Considering their size, some hotspots contained hundreds of genes, including many genes associated with immune responses and have been associated with AH (Table 2, Supplemental Tables 5 and 6). We performed pathway analysis on all of the genes in the hotspots and in regions with very significant changes in structure (all genes in Supplemental Table 4) and found that these regions are enriched for innate immune signaling (Figure 4B). Many of the hotspots contain large families of genes that are clustered together in the genome. For example, Chromosome 4 (~67-85M) contains the CXC-chemokines, Chromosome 5 (~140-145M) contains the protocadherins, and Chromosome 12 (~65-69M) contains IFNG, IL-22, and IL-26. One hotspot on Chromosome 19 (~34-56M) contains multiple large families of genes that are involved in diverse aspects of immune regulation including killer-cell immunoglobulin-like receptors (KIRs), leukocyte immunoglobulin-like receptors (LILRs), sialic-acid-binding immunoglobulin-like lectins (Siglecs), C5 complement receptors, and NOD-like family of receptors (NLRPs). Additionally, hotspots also contained other notable immune genes like NFKB1 (Chromosome 4), IFNGR1 (Chromosome 6), Integrin Beta (ITGB1) (Chromosome 1), and NFATC2 (Chromosome 20).

Structural Changes Observed at Innate Immune Gene Clusters are more complex than TADs

Because hotspots represent regions of the genome that have a large number of structural changes in disease, and they contain important genes involved in innate immunity, these regions were examined with finer detail. Within the hotspots, TAD structure, such as the loss or expansion of a TAD, was unchanged. Instead, most changes in genome architecture were due to the interaction profile within individual TADs and the relationship between the TADs and the surrounding genome.

CXC-chemokines are upregulated in AH, and we previously found increased co-regulation of these genes in response to LPS in AH patients, using single cell data of monocytes[20]. Zooming into the hotspot on chromosome 4 containing the CXC-chemokine cassette, we see that all of the CXC-chemokine genes exist within a single TAD (Figure 5). Interestingly, while the borders of the TAD did not change, the contact frequency within that TAD increased in AH. Zooming out, we observed an alternating pattern of interactions between this TAD and the neighboring TADs.

We previously found that monocytes in AH have increased expression of CLRs, which are a family of PRRs that sense a wide diversity of PAMPs and DAMPs. Many of these CLRs are found within the NK gene receptor complex on chromosome 12, and in particular, four of these CLRs (Mincle, Dectin-2, Dectin-3 and DCIR) are in close proximity and have highly co-regulated expression in AH. Similar to the CXC-chemokines, TAD structure in this hotspot did not change, but rather there were increased interactions within the individual TADs, increased connections between TADs within the entire NK-gene receptor complex (~7M-10M), and reduced interaction immediately outside of it

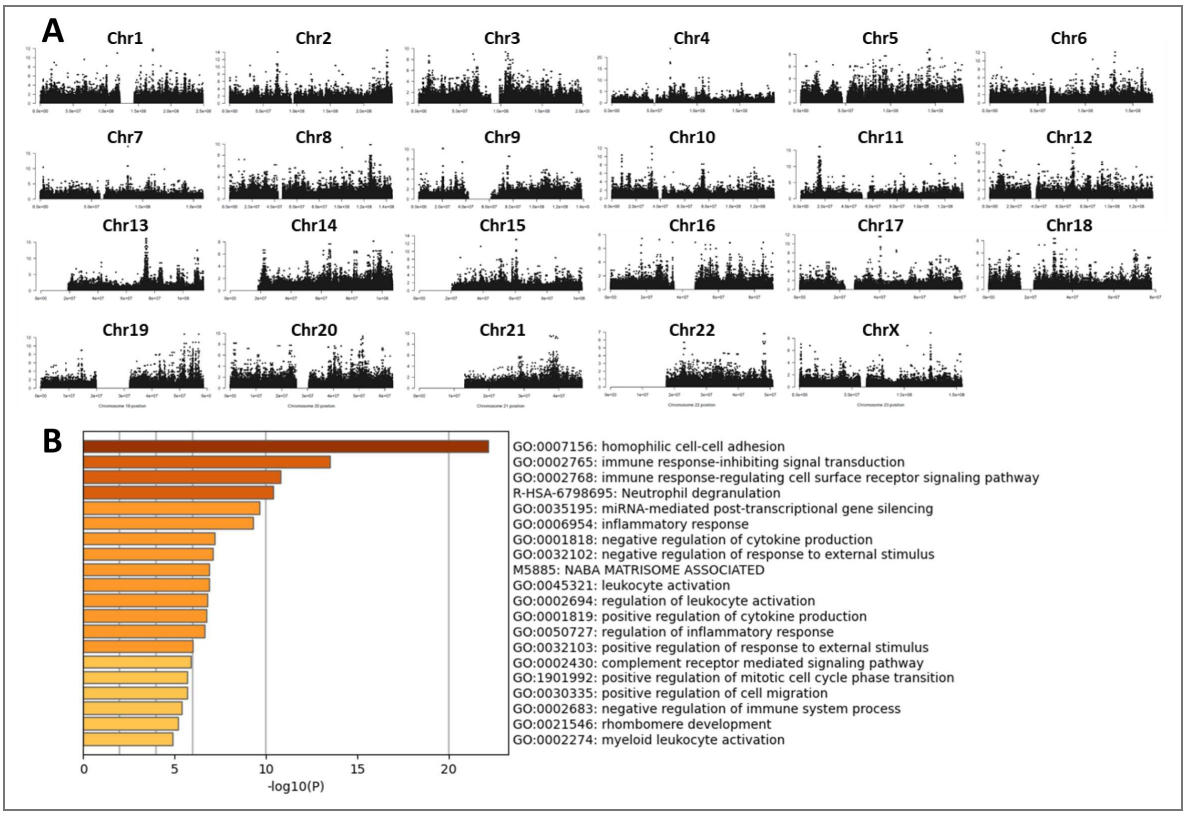

Figure 4. Certain Regions in the Genome have Hotspots of Significant Change in Disease

A)Manhattan plot showing regions of the genome with significant changes in chromatin interaction with disease. X-axis is position along the chromosome. Y-axis is –log10(p). B) Pathway analysis of genes in regions with the most significant changes with disease.

Table 2: Locations and gene contents of hotspots with significant change in AH			
Chromosome	**Range**	**Increased Frequency in AH**	**Decreased Frequency in AH**
Chr1	172M		DNM3, PIGC
Chr2	55M-75M	PSME4, ACYP2, GMCL1, SNRNP27, MXD1, CLEC4F, NAGK, ANXA1, DCTN1, DYSF	
Chr2	220M-241M	LINC01891, ARL4C, AGAP1	TRPM8, SPP2
Chr3	5M-20M	SYN2, TIMP4, MTCO1P5, IQSEC1, PPARG	
Chr3	105M-116M		ALCAM, CBLB, DIMT1P1, CD96, NECTIN3, DRD3
Chr4	67M-85M	CXCL1, CXCL5, CXCL6, CXCL8	CXCL1, CXCL5, CXCL6, CXCL8
Chr4	105M-116M	TBCK, AIMP1, ACTR6P1	NFKB1, CAMK2D
Chr5	140M-145M	PCDHA1, PCDHA2, PCDHA3, PCDHA4, PCDHA5, PCDHA6, PCDHA7, PCDHA8, PCDHA9, PCDHA10, PCDHA14, PCDHA11, PCDHA12, PCDHA13, PCDHB3, PCDHB4, PCDHB5, PCDHB6, PCDHB17P, PCDHB7, PCDHB8, PCDHB16, PCDHB9, PCDHB10, PCDHB11	FGF1,ARHGAP26,ARHGAP26-AS1
Chr6	127M-141M		L3MBTL3, SAMD3, TMEM200A, AKAP7, LOC100421246, RPL21P67, IFNGR1, RPS3AP23
Chr7	83M-89M	SEMA1A, SEMA3D, STEAP4	
Chr8	123M-130M		WASHC5, NSMCE2, RN7SL329P, TRIB1, RFPL4AP5, RNU11-4P
Chr10	8M-13M		ATP5F1C, TAF3, GATA3-AS1, GATA3
Chr10	30M-33M		NRP1, RN7SL63P, ITGB1, ITGB1-DT, MTND4LP11, RN7SL847P, RPL7AP53
Chr11	12M-17M	COPB1, PSMA1, PDE3B, CALCB, CALCP, CALCA, SOX6, INSC	FAR1, SPON1, RNA5SP332, RRAS2, CALCB, COPB1
Chr12	65M-69M		CAND1, MRPL40P1, IFNG-AS1, IFNG, NTAN1P3, LINC02420, MDM2, CPM, NUP107, KRT8P39, SLC35E3, IL22, IL26, MDM1
Chr13	66M-98M	UGGT2, HS6ST3, RN7SL164P, LINC00456	KLF12, RNU6-67P, SLITRK1
Chr13	108M-115M	LIG4, ABHD13, TNFSF13B, COL4A1, LINC00676, IRS2, COL4A2, COL4A2-AS1, RAB20	
Chr15	50M-62M	AP4E1, CYP19A1, MIR7973-1, GLDN, MIR4713HG, TNFAIP8L3, TMOD2, TMOD3, ALDH1A2, AQP9, MTCO3P23, MTND3P12, MTND4LP23, MTND5P32, MTCYBP23, ADAM10	DMXL2, LOC101928499, RPSAP55, ALDH1A2, AQP9, MTCO3P23, MTND3P12, MTND4LP23, MTND5P32, MTCYBP23, RORA, RORA-AS2, RNA5SP397
Chr17	39M-40M		PGAP3, ERBB2, MIEN1, GRB7, IKZF3, ZPBP2, CDC6, RARA, SMARCE1, KRT222, KRT224P, KRT24, KRT25, KRT26, KET27, KRT28
Chr18	23M-36M	DSC2, DSC3	
Chr19	34M-56M		LILRB1, LILRP2, KIR2DL3, KIR3DL3, KIR3DL1, KIR2DP1, KIR2DL1, KIR3DP1, SPACA6-AS1, SPACA6, HAS1, FPR1, FPR2, FPR3, NLRP12, MYADM, PRKCG, NCR1, NLRP7, NLRP2, NLRP13, NLRP8, NLRP5
Chr20	49M-51M		NFATC2, MIR3194, CEBPB-AS1, PELATON, LINC01270, ATP9A

Table 2. Locations and gene contents of hotspots with significant change in AH

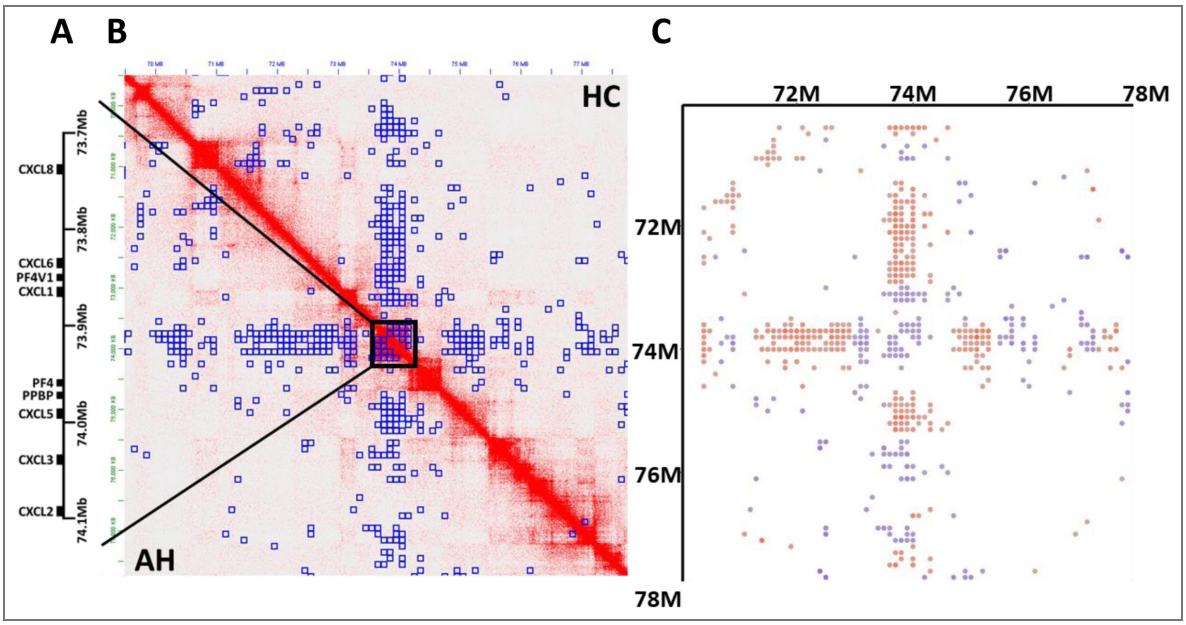

Figure 5. CXC-chemokine cluster has increase contact frequency within the TAD and reduced outside

A) Schematic of the CXC-chemokine gene cluster. **B)** Juicebox plot showing contact frequency map of the CXC-chemokine gene cluster and the surrounding genomic region. Blue boxes are 100kb regions significantly different in disease. **C)** Plot corresponding to the Juicebox plot showing whether each significant region increased (Blue) or decreased (Red) contact frequency in disease.

(Figure 6). Another hotspot on chromosome 12 at approximately 65-69M, which contains the genes for IL-22, IL-26, and IFNG, had the opposite structure, with fewer connections within the hotspot and more connections to the surrounding genomic landscape (Figure 7).

Two adjacent loci of CCL chemokine genes have increased connectivity and correlated expression

In AH, CC-chemokines are upregulated in monocytes, similar to CXC-chemokines and many other pro-inflammatory cytokines[20,27]. In the genome, the CC-chemokine genes are in two loci separated by about 1.5MB. From the Hi-C data, each CC-chemokine locus is within an individual TAD (Figure 8). While this region of the genome was not a hotspot, there was significant changes in 3D genome architecture, particularly in terms of the relationship between the CC-chemokine loci and the surrounding area, which increased connectivity in disease.

We previously published single-cell RNA-seq data from PBMCs isolated from patients with severe AH and healthy controls, with and without *ex vivo* LPS challenge (100pg/ml for 24 hours). In response to LPS, both HC and AH monocytes express chemokines, though the expression is much higher in AH. Next, we measured how well correlated gene expression was in single cells, in order to determine if neighboring genes have coordinated expression (Figure 8). In HC, we observed highly co-regulated expression of the CCL-chemokines in one of the loci (CCL3, CCL4, CCL3L1, CCL4L2). In AH, CCL-chemokine expression was highly co-regulated in both loci, including a few more genes in the first locus (CCL23, CCL18, CCL3, CCL4, CCL3L1, CCL4L2) and genes in the second locus (CCL2, CCL7, CCL13). And importantly, expression between both loci were also coordinated, suggesting the change in 3D genome architecture allowed for coordinated expression of these genes.

Discussion

Alcohol-associated Hepatitis is characterized by dysfunctional monocytes that increase systemic inflammation and can cause extensive damage to the liver and eventually end-organ failure. Monocytes from AH patients are hypersensitive to innate immune stimuli, and in response to bacterial LPS, upregulate expression of cytokines and chemokines much more dramatically than seen in healthy controls. In this study, we try to understand how changes in the 3D genome architecture of monocytes are transformed during AH and infer the impact these changes have on gene expression.

Many studies have been conducted trying to understand how changes in 3D genome architecture affects gene expression and cell development using unbiased and untargeted methods like Hi-C. Far fewer studies have been conducted on primary monocytes and how the architecture changes with disease. We hypothesized that in a disease like AH, where immune cells are so hypersensitive to LPS, alterations in 3D genome architecture may play a significant role in gene regulation. In our study, using monocytes isolated from four AH patients and 4 healthy controls, we in fact see significant changes in chromatin conformation caused by disease. But by measuring significant changes in contact frequency for every region-region pair, we were able to assess that throughout each chromosome, there were significant changes in how the TADs and larger loci associated with each other. Notably, we found a number of hotspots in the genome that contained a large number of structural changes.

Many large gene families and genes associated with innate immunity and AH were found within these hotspots. For example, in a previous publication, our group found highly coordinated expression of CXC-chemokines and some of the C-type lectin genes present within the NK-gene receptor complex[20]. Here, we find that the 3D genome architecture of these regions has significantly changed in disease. Moreover, throughout these hotspots we identified a number of other genes and gene families associated with AH. Chromosome 19 contained a large hotspot containing genes associated with the inflammasome (NOD-like receptors), which is an important

Figure 6. **Myeloid CLR gene cluster has increased local contacts in AH**

A) Schematic of the NK-gene receptor complex. **B)** Juicebox plot showing contact frequency map of the NK-gene receptor complex and the surrounding genomic region. Blue boxes are 100kb regions significantly different in disease. **C)** Plot corresponding to the Juicebox plot showing whether each significant region increased (Blue) or decreased (Red) contact frequency in disease.

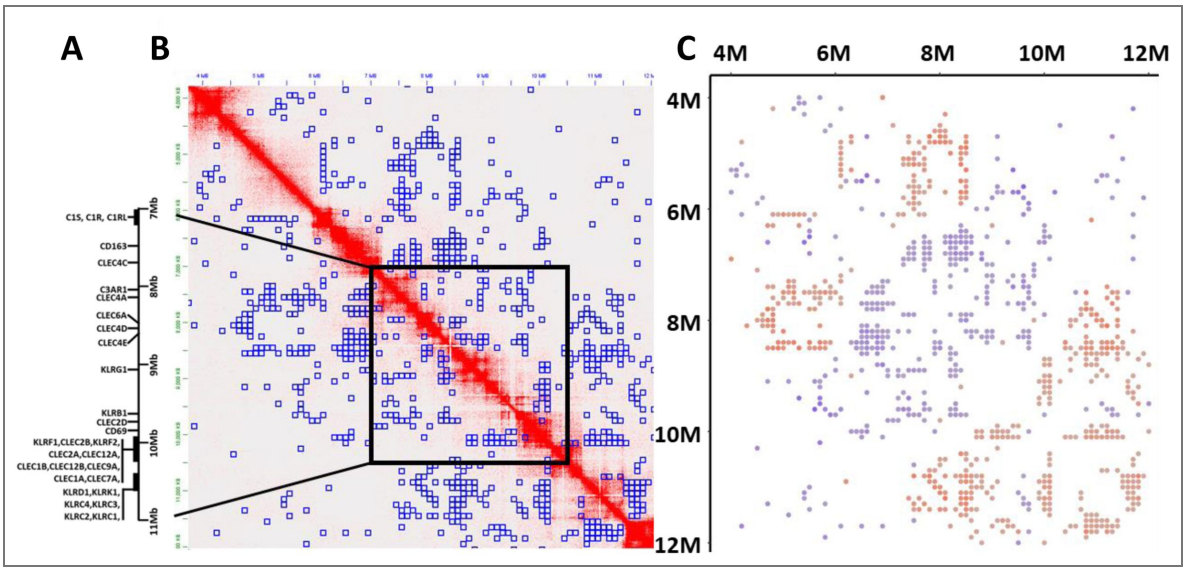

Figure 7. **Genomic region around IL-22 and IFNG have decreased local contacts in AH**

A) Juicebox plot showing contact frequency map of the region on Chromosome 12 around the IL-22 and IFNG genes. Blue boxes are regions significantly different in disease. **B)** Plot corresponding to the Juicebox plot showing whether each significant region increased (Blue) or decreased (Red) contact frequency in disease.

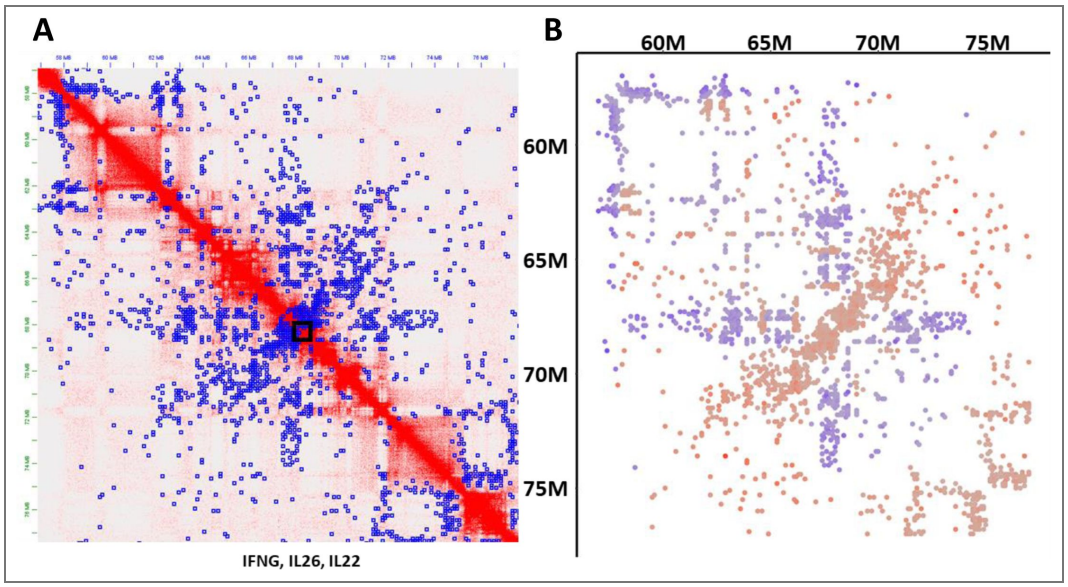

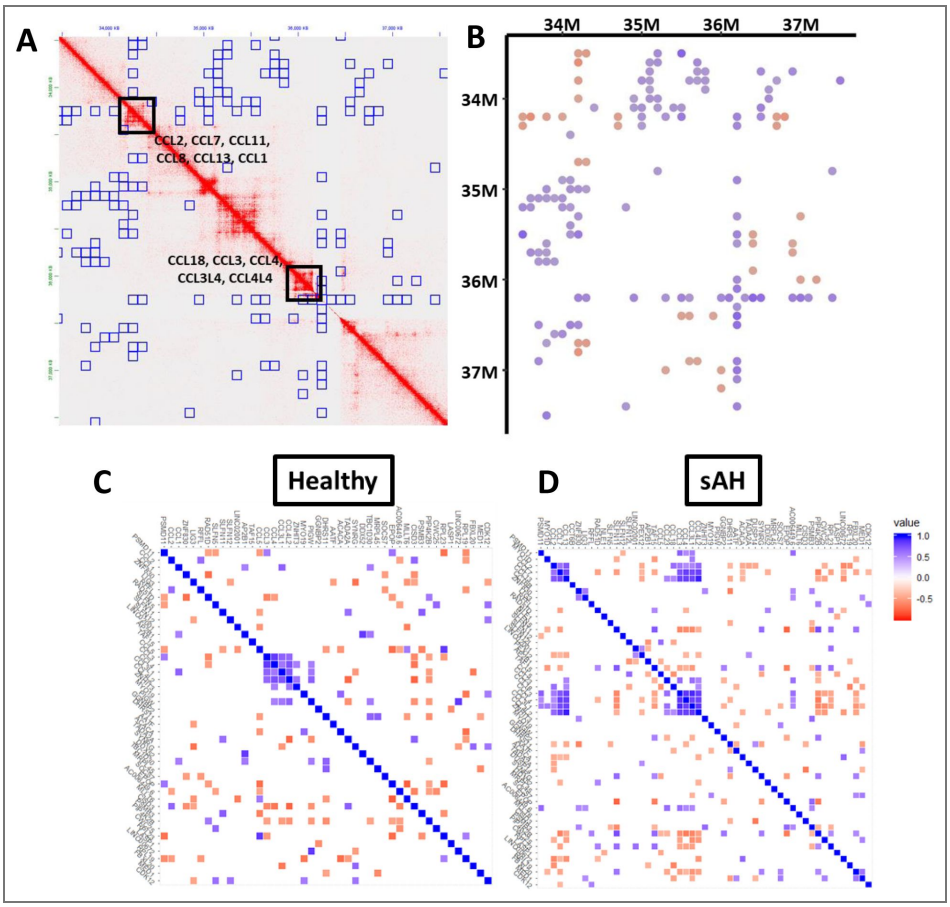

Figure 8. The Split CC-Chemokine Cluster has increased contact between loci, and highly correlated expression in AH

A) Juicebox plot showing contact frequency map of the two CC-chemokine gene clusters and the surrounding genomic region. Blue boxes are regions significantly different in disease. **B)** Plot corresponding to the Juicebox plot showing significantly increased (Blue) or decreased (Red) contact frequency in disease. **C/D)** Correlation analysis showing coordinately expressed in response to LPS (100pg/ml, for 24 hours) for healthy control (C) and AH (D). Genes are organized by chromosomal position and oriented in the same manner as A and B. Blue squares indicate genes with highly correlated expression while red squares indicate anti-correlated expression.

inflammatory complex involved in IL-1B release and pyroptosis, which contributes to significant damage in liver and other organs during AH[28,29]. This hotspot also contained SPACA6, which is a host gene for a cluster of microRNAs that are also upregulated in AH[30].

This region on chromosome 19 also contains the killer cell immunoglobulin-like receptor family, which are genes that encode transmembrane glycoproteins involved in NK-cell target recognition. Alongside the NK-gene receptor complex on Chromosome 12, another hotspot, our data suggests significant architectural changes in two different loci important for NK-cell target recognition in monocytes. While NK-cells are dysfunctional in AH[31,32], the structural changes we observe in monocytes in these regions is more likely to do with the other gene families in the area, such as in the chromosome 12 hotspot, the CLR genes, and in the chromosome 19 hotspot, the leukocyte immunoglobulin-like receptors, which are highly coordinately expressed in monocytes.

On the other hand, some of the hotspots contained genes with unclear roles in monocytes or AH. Looking at single cell data, some of these hotspots contained genes with very low expression in monocytes. For example, the T-cell receptor locus on chromosome 14, which increased contact frequency throughout the length of the chromosome, but none of these genes are expressed in monocytes. But all of these hotspots are more than just the genes within and may contain important regulatory elements.

While the CC-chemokine gene cassettes on chromosome were not a clear hotspot with a large number of changes in disease, there were still significant differences. This region was of interest because many CCL chemokines are highly upregulated in response to LPS in AH patients[20], and levels of circulating CCL chemokines are higher in disease[33]. In AH, the two CC-chemokine cassettes, which are separated by a little more than 1Mb and are in different TADs, had higher contact frequency and from single-cell data, had highly correlated expression. This suggests that these two regions came closer together in disease, and that the proximity of regulatory elements had an effect on the expression of these genes.

While there were significant changes in 3D genome architecture in AH, this study has a number of limitations. Other Hi-C studies in monocytes and THP-1 cells have been limited by small sample size, typically one patient/sample or two patients with the data combined to increase resolution. This is not ideal for human disease which is typically multifactorial and complex. In this study, we studied monocytes isolated from four healthy controls and four AH patients, in order to look at changes in contact frequency with high statistical confidence. But the trade-off was that we could not analyze this data at a much higher resolution without much deeper sequencing. Still, to fully understand how genome architecture changes with disease, even more patient samples need to be sequenced and analyzed with Hi-C, to encompass the multifactorial nature of this complex human disease.

Taken together, these results indicate that the 3D genome architecture of monocytes is significantly altered in AH and suggest that perturbations in the 3D architecture contribute to differences in gene expression, especially in response to innate immune challenges. Future studies will focus on trying to understand the cause of genome restructuring in AH, as both alcohol and innate immune stimuli have the potential to alter epigenetic gene regulation[34]. Additionally, more work is needed to understand how changes in local genome structure affect transcription factor dynamics and the relationship of enhancers and promoters in disease. Finally, these studies suggest that Hi-C is a useful tool to understand how disease alters the genome, and there is an ongoing need to build more databases of this kind of data from a wider diversity of cell types, disease states, and patients.

Methods

Alcohol-related Hepatitis and Healthy Control Patient Selection

Enrolled patients had confirmed diagnosis of AH by clinicians at the Cleveland Clinic based on medical history, physical examination, and laboratory results, according to the guidelines of the American College of Gastroenterology [*https://gi.org/clinical-guidelines/*] (Supplemental Table

1). Healthy controls were recruited from the Clinical Research Unit at the Cleveland Clinic.

Isolation of Human PBMCs

PBMCs were isolated from human blood as previously described[20,30]. Isolation of mononuclear cells was performed by density gradient centrifugation on Ficoll-Paque PLUS (GE Healthcare, Uppsala, Sweden). 1 mL of freshly collected Buffy Coat was mixed at a ratio of 1:5 (vol/vol) with phosphate buffered saline (PBS) at 37°C and divided and layered onto 8 mL Ficoll-Paque PLUS in two 15 mL conical centrifuge tubes. After centrifugation at 400 × g for 30 min at 20°C (no brake), buffy coat fractions were collected, pooled, resuspended in culture media (Roswell Park Memorial Institute (RPMI)-1640 supplemented with 100 µM Penicillin-streptomycin and 10% fetal bovine serum (FBS)), and centrifuged at 400 × g for 15 min at 20°C. The pellets were resuspended in 8 mL of culture media, counted, and again centrifuged at 400 × g for 8 min at 20°C. Cells were then cryopreserved by resuspending in freezing media (50% culture media, 40% FBS, 10% dimethyl sulfoxide (DMSO)) at a concentration of 1.5×10^6 cells/mL, and allowed to freeze slowly to −80°C in a styrofoam container. For long-term preservation, cells were stored in liquid nitrogen.

Hi-C of Isolated Monocytes from Cryopreserved PBMCs

Cryopreserved PBMCs from 4 AH patients and 4 age-matched healthy controls were thawed following the 10x protocol for cryopreserved PBMCs. Monocytes were isolated by negative selection using the EasySep Human Monocyte Enrichment Kit without CD16 Depletion (StemCell Technologies, Cambridge, MA) according to factory instructions. Hi-C was performed with the Arima Genome-wide Hi-C kit (Carlsbad, CA) according to factory instructions. Libraries were pooled and sequenced with an Illumina Novaseq 6000.

Analysis of Hi-C Data

Sequencing data for the Hi-C experiments were aligned to the genome (GRC38, release 93) using Juicer[35]. From the output of Juicer, we summarized the quality of the Hi-C maps using the inter.txt files (Supplementary Table 2). Chromosomal correlations were calculated using HiCRep[23]. Differential contact frequencies were measured using multiHiCcompare, at a resolution of 100kb and using the inter.hic files from Juicer[24]. Hi-C data was visualized using Juicebox to view each of the inter.hic files[36]. Regions with changes in contact frequency in disease were labeled using data from multiHiCcompare. To ensure these changes in contact frequency are due to disease and not random chance, we randomized the samples and recalculated differential contact frequency and found significantly fewer differences (Supplemental Table 3).

"Hotspots" were defined as regions of the genome with a high frequency of changes in contact frequency. To identify these regions, we took the list of all differential contacts from multiHiCcompare and filtered by a very stringent statistical cutoff of padj<0.0000001. Then we identified regions of the genome with a large number of these differential contacts, which identified 22 "hotspots" (Table 2, Supplemental Table 4). To identify the borders of these regions, we looked more liberally at the full list of differential contacts (padj<0.05). Gene enrichment for genes present in hotspots and other highly differential regions was performed using Metascape[37].

scRNA-seq Analysis and Clustering

Sequencing data was aligned to the Human genome (GRC38, release 93) using cellranger (v3.0.2). All gene expression and clustering analyses were performed using Seurat (3.1.1) as previously described[20,38]. Briefly, all samples were first normalized using SCTransform and then filtered to remove low quality cells (nFeature_RNA<4000, nFeature_RNA>200, percent.mt<20, which removes doublets, cells with low reads, and cells with high mitochondrial content))[39]. All samples were combined using the PrepSCTIntegration and FindIntegrationAnchors functions to find common anchor genes in all samples for all cell types, and then integrated using the IntegrateData function, with all normalizations using the SCT transformed data[38,40]. Clustering was performed using RunPCA and RunUMAP, and clusters were identified using FindNeighbors and FindClusters.

bigSCale2

For correlation analyses, bigSCale2 was used to calculate correlations using the Z-score algorithm[41]. For these analyses, only monocytes were used (clusters labeled CD14_Monocyte1, CD14_Monocyte2, CD14_Monocyte3, and CD16_Monocyte). All gene clusters were determined by first ordering all annotated human genes by chromosome and start codon then finding the desired clusters and selecting an arbitrary set of genes surrounding it (genes that are not hypothesized to be involved) to ensure the entire cluster was obtained. Genes were then filtered for low expression using the criteria that bigSCale2 was unable to determine a correlation coefficient. Heatmaps of the correlation coefficients were made with only the top and bottom 5% of all correlation coefficients shown, to remove noise and isolate the most important correlations.

Data availability

The Hi-C data generated for this study can be found at the database of Genotypes and Phenotypes (dbGaP) [TBD] The scRNA-seq data for this study can be found at National Center for Biotechnology Information Gene Expression Omnibus under accession number [PRJNA596980]20. All scripts used for analyses, differential expression results, for all cell types, and figure generation can be found at the author's github (*https://github.com/atomadam2/*). Any additional information required to reanalyze the data reported in this paper is available from the lead contact upon request.

Acknowledgements

The authors thank the Clinical Research Unit, Genomics Core and Computing Services at the Cleveland Clinic. Additionally, Dr. Laura E Nagy, from the Cleveland Clinic and Northern Ohio Alcohol Center, for reagents and critical comments on the manuscript.

Additional information

Ethical Approval and Consent to Participate

The study protocol was approved by the Institutional Review Board for the Protection of Human Subjects in Research at the Cleveland Clinic and MetroHealth Hospitals, Cleveland. All methods were performed in accordance with the IRB's guidelines and regulations and written informed consent was obtained from all subjects.

Author Contributions

AK contributed conception and design of the study. MRM helped conduct the experiments. JD, AB, DS, NW, SD recruited patients and performed clinical analyses. AK analyzed the data and wrote the first draft of the manuscript. All authors contributed to manuscript revision, read and approved the submitted version.

Financial Support

This work was funded by the following NIH-NIAAA grants: K99/R00AA028048 (AK), R01GM119174, R01DK113196, U01AA021890, U01AA026976, R56HL141744, U01DK061732, U01DK062470, R21AR071046 (SD), K12HL141952, American College of Gastroenterology Clinical Research Award, K08AAAA028794 (NW).

Funding

Funder	Grant reference number	Author
HHS | NIH | National Institute on Alcohol Abuse and Alcoholism (NIAAA)	R00AA028048	Adam Kim

HHS | NIH | National Institute of General Medical Sciences (NIGMS)	R01GM119174	Srinivasan Dasarathy
HHS | NIH | National Institute of Diabetes and Digestive and Kidney Diseases (NIDDK)	R01DK113196	Srinivasan Dasarathy
HHS | NIH | National Institute on Alcohol Abuse and Alcoholism (NIAAA)	U01AA021890	Srinivasan Dasarathy
HHS | NIH | National Institute on Alcohol Abuse and Alcoholism (NIAAA)	U01AA026976	Srinivasan Dasarathy
HHS | NIH | National Heart, Lung, and Blood Institute (NHLBI)	R56HL141744	Srinivasan Dasarathy
HHS | NIH | National Institute of Diabetes and Digestive and Kidney Diseases (NIDDK)	U01DK061732	Srinivasan Dasarathy
HHS | NIH | National Institute of Diabetes and Digestive and Kidney Diseases (NIDDK)	U01DK062470	Srinivasan Dasarathy
HHS | NIH | National Institute on Aging (NIA)	R21AR071046	Srinivasan Dasarathy
HHS | NIH | National Heart, Lung, and Blood Institute (NHLBI)	K12HL141952	Nicole Welch
HHS | NIH | National Institute on Alcohol Abuse and Alcoholism (NIAAA)	K08AA028794	Nicole Welch

Author ORCID iDs

Adam Kim: https://orcid.org/0000-0002-3186-3912
Srinivasan Dasarathy: https://orcid.org/0000-0003-1774-0104

Additional files

Supplemental Tables.

References

1 **Cremer T.,** Cremer C (2001) Chromosome territories, nuclear architecture and gene regulation in mammalian cells. *Nat Rev Genet* **2**:292-301 https://doi.org/10.1038/35066075 | PubMed

2 **Szabo Q.,** Bantignies F., Cavalli G (2019) Principles of genome folding into topologically associating domains. *Sci Adv* **5**:eaaw1668 https://doi.org/10.1126/sciadv.aaw1668 | PubMed

3 **Sanborn A. L.,** et al. (2015) Chromatin extrusion explains key features of loop and domain formation in wild-type and engineered genomes. *Proc Natl Acad Sci U S A* **112**:E6456-6465 https://doi.org/10.1073/pnas.1518552112 | PubMed

4 **Vietri Rudan M,** et al. (2015) Comparative Hi-C reveals that CTCF underlies evolution of chromosomal domain architecture. *Cell Rep* **10**:1297-1309 https://doi.org/10.1016/j.celrep.2015.02.004 | PubMed

5 **Rao S. S. P.,** et al. (2017) Cohesin Loss Eliminates All Loop Domains. *Cell* **171**:305-320.e324 https://doi.org/10.1016/j.cell.2017.09.026 | PubMed

6 **Nora E. P.,** et al. (2017) Targeted Degradation of CTCF Decouples Local Insulation of Chromosome Domains from Genomic Compartmentalization. *Cell* **169**:930-944.e922 https://doi.org/10.1016/j.cell.2017.05.004 | PubMed

7 **Schwarzer W.,** et al. (2017) Two independent modes of chromatin organization revealed by cohesin removal. *Nature* **551**:51-56 https://doi.org/10.1038/nature24281 | PubMed

8 **Stik G.,** et al. (2020) CTCF is dispensable for immune cell transdifferentiation but facilitates an acute inflammatory response. *Nat Genet* **52**:655-661 https://doi.org/10.1038/s41588-020-0643-0 | PubMed

9 **Yang B.,** et al. (2023) CTCF controls three-dimensional enhancer network underlying the inflammatory response of bone marrow-derived dendritic cells. *Nat Commun* **14**:1277 https://doi.org/10.1038/s41467-023-36948-5 | PubMed

10 **Kolovos P.,** et al. (2016) Binding of nuclear factor kappaB to noncanonical consensus sites reveals its multimodal role during the early inflammatory response. *Genome Res* **26**:1478-1489 https://doi.org/10.1101/gr.210005.116 | PubMed

11 **Liu R.,** et al. (2024) Hi-C, a chromatin 3D structure technique advancing the functional genomics of immune cells. *Front Genet* **15** https://doi.org/10.3389/fgene.2024.1377238 | PubMed

12 **Cuartero S.,** Stik G., Stadhouders R (2023) Three-dimensional genome organization in immune cell fate and function. *Nat Rev Immunol* **23**:206-221 https://doi.org/10.1038/s41577-022-00774-5 | PubMed

13 **Platanitis E.,** et al. (2022) Interferons reshape the 3D conformation and accessibility of macrophage chromatin. *iScience* **25** https://doi.org/10.1016/j.isci.2022.103840 | PubMed

14 **Minderjahn J.,** et al. (2022) Postmitotic differentiation of human monocytes requires cohesin-structured chromatin. *Nat Commun* **13**:4301 https://doi.org/10.1038/s41467-022-31892-2 | PubMed

15 **Xia Y.,** et al. (2022) Capturing 3D Chromatin Maps of Human Primary Monocytes: Insights From High-Resolution Hi-C. *Front Immunol* **13** https://doi.org/10.3389/fimmu.2022.837336 | PubMed

16 **Zhang Z.,** et al. (2020) Massive reorganization of the genome during primary monocyte differentiation into macrophage. *Acta Biochim Biophys Sin* **52**:546-553 https://doi.org/10.1093/abbs/gmaa026 | PubMed

17 **Liu Y.,** Li H., Czajkowsky D. M., Shao Z (2021) Monocytic THP-1 cells diverge significantly from their primary counterparts: a comparative examination of the chromosomal conformations and transcriptomes. *Hereditas* **158** https://doi.org/10.1186/s41065-021-00205-w | PubMed

18 **Wang M.,** et al. (2014) Chronic alcohol ingestion modulates hepatic macrophage populations and functions in mice. *J Leukoc Biol* **96**:657-665 https://doi.org/10.1189/jlb.6A0114-004RR | PubMed

19 **Ju C.,** Mandrekar P (2015) Macrophages and Alcohol-Related Liver Inflammation. *Alcohol Res* **37**:251-262 https://doi.org/10.35946/arcr.v37.2.09 | PubMed

20 **Kim A.,** Bellar A., McMullen M. R., Li X., Nagy L. E (2020) Functionally Diverse Inflammatory Responses in Peripheral and Liver Monocytes in Alcohol-Associated Hepatitis. *Hepatol Commun* **4**:1459-1476 https://doi.org/10.1002/hep4.1563 | PubMed

21 **Wu X.,** et al. (2023) Recent Advances in Understanding of Pathogenesis of Alcohol-Associated Liver Disease. *Annu Rev Pathol* **18**:411-438 https://doi.org/10.1146/annurev-pathmechdis-031521-030435 | PubMed

22 **Liu M.,** et al. (2021) Super enhancer regulation of cytokine-induced chemokine production in alcoholic hepatitis. *Nat Commun* **12**:4560 https://doi.org/10.1038/s41467-021-24843-w | PubMed

23 **Yang T.,** et al. (2017) HiCRep: assessing the reproducibility of Hi-C data using a stratum-adjusted correlation coefficient. *Genome Res* **27**:1939-1949 https://doi.org/10.1101/gr.220640.117 | PubMed

24 **Stansfield J. C.,** Cresswell K. G., Dozmorov M. G (2019) multiHiCcompare: joint normalization and comparative analysis of complex Hi-C experiments. *Bioinformatics* **35**:2916-2923 https://doi.org/10.1093/bioinformatics/btz048 | PubMed

25 **Burton J. N.,** et al. (2013) Chromosome-scale scaffolding of de novo genome assemblies based on chromatin interactions. *Nat Biotechnol* **31**:1119-1125 https://doi.org/10.1038/nbt.2727 | PubMed

26 **Lieberman-Aiden E.,** et al. (2009) Comprehensive mapping of long-range interactions reveals folding principles of the human genome. *Science* **326**:289-293 https://doi.org/10.1126/science.1181369 | PubMed

27 **Degre D.,** et al. (2012) Hepatic expression of CCL2 in alcoholic liver disease is associated with disease severity and neutrophil infiltrates. *Clin Exp Immunol* **169**:302-310 https://doi.org/10.1111/j.1365-2249.2012.04609.x | PubMed

28 **Khanova E.,** et al. (2018) Pyroptosis by caspase11/4-gasdermin-D pathway in alcoholic hepatitis in mice and patients. *Hepatology* **67**:1737-1753 https://doi.org/10.1002/hep.29645 | PubMed

29 **Petrasek J.,** et al. (2012) IL-1 receptor antagonist ameliorates inflammasome-dependent alcoholic steatohepatitis in mice. *J Clin Invest* **122**:3476-3489 https://doi.org/10.1172/JCI60777 | PubMed

30 **Kim A.,** Saikia P., Nagy L. E (2019) miRNAs Involved in M1/M2 Hyperpolarization Are Clustered and Coordinately Expressed in Alcoholic Hepatitis. *Frontiers in Immunology* **10** https://doi.org/10.3389/fimmu.2019.01295 | PubMed

31 **Kim A.,** et al. (2022) Diminished function of cytotoxic T- and NK-cells in severe alcohol-associated hepatitis. *Metabolism and Target Organ Damage* **2** https://doi.org/10.20517/mtod.2022.13 | PubMed

32 **Stoy S.,** et al. (2015) Cytotoxic T lymphocytes and natural killer cells display impaired cytotoxic functions and reduced activation in patients with alcoholic hepatitis. *Am J Physiol Gastrointest Liver Physiol* **308**:G269-276 https://doi.org/10.1152/ajpgi.00200.2014 | PubMed

33 **Luther J.,** Vannier A. G., Schaefer E. A., Goodman R. P (2022) The circulating proteomic signature of alcohol-associated liver disease. *JCI Insight* **7** https://doi.org/10.1172/jci.insight.159775 | PubMed

34 **Malherbe D. C.,** Messaoudi I (2022) Transcriptional and Epigenetic Regulation of Monocyte and Macrophage Dysfunction by Chronic Alcohol Consumption. *Front Immunol* **13** https://doi.org/10.3389/fimmu.2022.911951 | PubMed

35 **Durand N. C.,** et al. (2016) Juicer Provides a One-Click System for Analyzing Loop-Resolution Hi-C Experiments. *Cell Syst* **3**:95-98 https://doi.org/10.1016/j.cels.2016.07.002 | PubMed

36 **Robinson J. T.,** et al. (2018) Juicebox.js Provides a Cloud-Based Visualization System for Hi-C Data. *Cell Syst* **6**:256-258.e251 https://doi.org/10.1016/j.cels.2018.01.001 | PubMed

37 **Zhou Y.,** et al. (2019) Metascape provides a biologist-oriented resource for the analysis of systems-level datasets. *Nat Commun* **10**:1523 https://doi.org/10.1038/s41467-019-09234-6 | PubMed

38 **Stuart T.,** et al. (2019) Comprehensive Integration of Single-Cell Data. *Cell* **177**:1888-1902.e1821 https://doi.org/10.1016/j.cell.2019.05.031 | PubMed

39 **Hafemeister C.,** Satija R (2019) Normalization and variance stabilization of single-cell RNA-seq data using regularized negative binomial regression. *Genome Biol* **20** https://doi.org/10.1186/s13059-019-1874-1 | PubMed

40 **Ding J.,** et al. (2019) Systematic comparative analysis of single cell RNA-sequencing methods. *bioRxiv* https://doi.org/10.1101/632216

41 **Iacono G.,** Massoni-Badosa R., Heyn H (2019) Single-cell transcriptomics unveils gene regulatory network plasticity. *Genome Biol* **20** https://doi.org/10.1186/s13059-019-1713-4 | PubMed

Peer reviews

Reviewer #3 (Public review):

In this manuscript, the authors use HiC to study the 3D genome of CD14+ CD16+ monocytes from the blood of healthy and those from patients with Alcohol-associated Hepatitis.

Overall, the authors perform a cursory analysis of the HiC data and conclude that there are a large number of changes in 3D genome architecture between healthy and AH patient monocytes. They highlight some specific examples that are linked to changes in gene expression. The analysis is of such a preliminary nature that I would usually expect to see the data from all figures in just one or two figures.

In addition, I have a number of concerns regarding the experimental design and the depth of the analyses performed that I think must be addressed.

(1) There is a myriad of literature that describes the existence of cell-type-specific 3D genome architecture. In this manuscript, there is an assumption by the authors that the CD14+ CD16+

monocytes represent the same population from both the healthy and diseased patients. Therefore, the authors conclude that the differences they see in the HiC data are due to disease-related changes in the equivalent cell types. However, I am concerned that the AH patient monocytes may have differentiated due to their environment so that they are in fact akin to a different cell type and the 3D genome changes they describe reflect this. This is supported by published articles, for example: Dhanda et al., Intermediate Monocytes in Acute Alcoholic Hepatitis Are Functionally Activated and Induce IL-17 Expression in CD4+ T Cells. J Immunol (2019) 203 (12): 3190-3198, in which they show an increased frequency of CD14+ CD16+ intermediate monocytes in AH patients that are functionally distinct.

I suggest that if the authors would like to study the specific effects of AH on 3D genome architecture then they should carefully FACsort the equivalent monocyte populations from the healthy and AH patients.

(2) The analysis of the HiC data is quite preliminary. In the 3D genome field, it is usual to report the different scales of genome architecture, for example, compartments, topologically associated domains (TADs) and loops. I think that reporting this information and how it changes in AH patients in the appropriate cell types would be of great interest to the field.

Comments on revisions:

In the revision the authors did not respond to my concerns which I believe still remain valid and compromise the author's conclusions of AH-specific effects on genome architecture.

https://doi.org/10.7554/eLife.102626.2.sa1

Author response:

The following is the authors' response to the original reviews.

> ***Public Reviews:***
>
> ***Reviewer #1 (Public review):***
>
> *Summary:*
>
> *The authors investigate the relationship between 3D chromatin architecture and innate immune gene regulation in monocytes from patients with alcohol-associated hepatitis (AH). Using Hi-C technology, they attempt to identify structural changes in the genome that correlate with altered gene expression. Their central claim is that genome restructuring contributes to the hyper-inflammatory phenotype associated with AH.*
>
> *Strengths:*
>
> *(1) The manuscript employs Hi-C technology, which, in principle, is a powerful approach for studying genome organization.*
>
> *(2) The focus on disease-relevant genes, particularly innate immune loci, provides a contextually important angle for understanding AH.*
>
> *Weaknesses:*
>
> *(1) Sample Size: The study relies on an exceptionally small cohort (4 AH patients and 4 healthy controls), rendering the results statistically underpowered and highly susceptible to variability.*
>
> *(2) Hi-C Resolution unpaired to RNA seq: The data are presented at a resolution of 100kb, which is insufficient to uncover meaningful chromatin interactions at the level of*

individual genes. This data is unpaired.

(3) Functional Validation: The manuscript lacks experiments to directly link changes in chromatin architecture with gene expression or monocyte function, leaving the claims speculative.

(4) Data Integration: The lack of Hi-C with ATAC and RNA-seq data handicaps the analysis and really makes it superficial. In short, it does not convincingly demonstrate a functional relationship.

(5) Confounding Factors: The manuscript neglects critical confounding variables such as comorbidities, medications, and lifestyle factors, which could influence chromatin structure and gene expression independently of AH.

Appraisal of the Aims and Results:

The manuscript sets out to establish a connection between chromatin architecture and AH pathology. However, the study fails to achieve its stated aims due to inadequate methods and insufficient data. The conclusions drawn from the Hi-C analyses alone are poorly supported, and the lack of functional validation undermines the credibility of the proposed mechanisms. Overall, the results do not provide compelling evidence to substantiate the authors' claims.

Impact on the Field and Utility to the Community:

The work, in its current form, is unlikely to have a meaningful impact on the field. The limited scope, methodological shortcomings, and lack of robust data significantly diminish its potential utility. Without addressing these critical gaps, the study does not offer new insights into the role of genome architecture in AH or provide useful methodologies or datasets for the community.

Additional Context:

The manuscript would benefit from a more comprehensive analysis of potential mechanisms underlying the observed changes, including the interplay between chromatin architecture and epigenetic modifications. Furthermore, longitudinal studies or therapeutic interventions could provide insights into the dynamic aspects of genome restructuring in AH. These considerations are entirely absent from the current study.

Conclusion:

The manuscript does not achieve its stated goals and does not present sufficient evidence to support its conclusions. The limitations in sample size, resolution, and experimental rigor severely hinder its contribution to the field. Addressing these fundamental flaws will be essential for the work to be considered a meaningful addition to the literature.

Reviewer #2 (Public review):

Summary:

Dr. Adam Kim and collaborators study the changes in chromatin structure in monocytes obtained from alcohol-associated hepatitis (AH) when compared to healthy controls (HC). Through the usage of high throughput chromatin conformation capture technology (Hi-C), they collected data on contact frequencies between both contiguous and distal DNA windows (100 kB each); mainly within the same chromosome. From the analyses of those data in the two cohorts under analysis, authors describe frequent pairs of regions subject to significant changes in contact frequency across cohorts. Their accumulation onto specific regions of the genome -referred to as hotspots- motivated authors to narrow

down their analyses to these disease-associated regions, in many of which, authors claim, a number of key innate immune genes can be found. Ultimately, the authors try to draw a link between the changes observed in chromatin architecture in some of these hotspots and the differential co-expression of the genes lying within those regions, as ascertained in previous single-cell transcriptomic analyses.

Strengths:

The main strength of this paper lies in the generation of Hi-C data from patients, a valuable asset that, as the authors emphasize, offers critical insights into the role of chromatin architecture dysregulation in the pathogenesis of alcohol-associated hepatitis (AH). If confirmed, the reported findings have the potential to highlight an important, yet overlooked, aspect of cellular dysregulation-chromatin conformation changes - not only in AH but potentially in other immune-related conditions with a component of pathological inflammation.

Weaknesses:

In what I regard as the two most important weaknesses of the work, I feel that they are more methodological than conceptual. The first of these issues concerns the perhaps insufficient level of description provided on the definition of some key types of genomic regions, such as topologically associated domains, DNA hotspots, or even DNA loci showing significant changes in contact frequency between AH and HC. In spite of the importance of these concepts in the paper, no operational, explicit description of how are they defined, from a statistical point of view, is provided in the current version of the manuscript.

Without these definitions, some of the claims that authors make in their work become hard to sustain. Some examples are the claim that randomizing samples does not lead to significant differences between cohorts; the claim that most of the changes in contact frequency happen locally; or the claim that most changes do not alter the structure of TADs, but appear either within, or between TADs. In my viewpoint, specific descriptions and implementation of proper tests to check these hypotheses and back up the mentioned specific claims, along with the inclusion of explicit results on these matters, would contribute very significantly to strengthening the overall message of the paper.

The second notable weakness of the study pertains to the characterization of the changes observed around immune genes in relation to genome-wide expectations. Although the authors suggest that certain hotspots contain a high number of immune-related genes, no enrichment analysis is provided to verify whether these regions indeed harbor a higher concentration of such genes compared to other genomic areas. It would be important for readers to be promptly informed if no such enrichment is observed, for in that case, the presence of some immune genes within these hotspots would carry more limited implications.

Additionally, the criteria used to define a hotspot are not clearly outlined, making it difficult to assess whether the changes in contact frequencies around the immune genes highlighted in figures 5-8 are truly more pronounced than what would be expected genome-wide.

Reviewer #3 (Public review):

In this manuscript, the authors use HiC to study the 3D genome of CD14+ CD16+ monocytes from the blood of healthy and those from patients with Alcohol-associated Hepatitis.

Overall, the authors perform a cursory analysis of the HiC data and conclude that there are a large number of changes in 3D genome architecture between healthy and AH patient monocytes. They highlight some specific examples that are linked to changes in gene expression. The analysis is of such a preliminary nature that I would usually expect to see the data from all figures in just one or two figures.

In addition, I have a number of concerns regarding the experimental design and the depth of the analyses performed that I think must be addressed.

(1) There is a myriad of literature that describes the existence of cell type-specific 3D genome architecture. In this manuscript, there is an assumption by the authors that the CD14+ CD16+ monocytes represent the same population from both healthy and diseased patients. Therefore, the authors conclude that the differences they see in the HiC data are due to disease-related changes in the equivalent cell types. However, I am concerned that the AH patient monocytes may have differentiated due to their environment so that they are in fact akin to a different cell type and the 3D genome changes they describe reflect this. This is supported by published articles for example: Dhanda et al., Intermediate Monocytes in Acute Alcoholic Hepatitis Are Functionally Activated and Induce IL-17 Expression in CD4+ T Cells. J Immunol (2019) 203 (12): 3190-3198, in which they show an increased frequency of CD14+ CD16+ intermediate monocytes in AH patients that are functionally distinct.

I suggest that if the authors would like to study the specific effects of AH on 3D genome architecture then they should carefully FACsort the equivalent monocyte populations from the healthy and AH patients.

(2) The analysis of the HiC data is quite preliminary. In the 3D genome field, it is usual to report the different scales of genome architecture, for example, compartments, topologically associated domains (TADs), and loops. I think that reporting this information and how it changes in AH patients in the appropriate cell types would be of great interest to the field.

We thank the reviewers for their careful and thorough examination of our manuscript. We agree with all of their comments regarding the limitations of the study. Many of the criticisms focus on the small sample size of our study (n=4 for healthy controls and disease patients) in both Hi-C and single-cell RNA-seq experiments, and that these experiments are unpaired, or in other words, PBMCs came from different patients for each experiment.

Unfortunately, these experiments are fairly complicated to perform, requiring patient cells and very expensive deep sequencing. We are not currently in a position to be able to easily or cost effectively increase sample size. In the case of Hi-C, we still believe our study to be of value as Hi-C is not a commonly used technique to study disease effects on chromatin, and very few studies have employed a large enough sample size to perform statistical comparisons. Additionally, to analyze the data at a higher resolution would require deeper sequencing, and unfortunately we do not have the resources to sequence these libraries deeper. Regarding the single-cell RNA-seq data, this dataset was generated for an earlier study [1] focusing on gene expression responses to LPS, and we were unable to get PBMCs from exactly the same patients to perform the Hi-C study.

We disagree that our study has limited scientific value. Our study is the first to use Hi-C to show that the 3D genome architecture of primary monocytes is changed in a disease context. The only other study to follow a similar approach performed Hi-C in monocytes from 2 healthy and 2 Systemic lupus erythematosus (SLE) patients, and in their study the data from both patients were combined prior to comparison. No statistics were performed and their conclusion was no differences in genome architecture due to disease. They did find

differences between primary monocytes and the THP1 monocytic cell line, but this lacked statistical analysis. Their conclusion was that inflammatory disease may not lead to genome wide changes in architecture. Our study, though a very different disease than SLE, shows statistically significant differences between AH and healthy controls. We believe our study lays the groundwork for how Hi-C can be used to study genome architecture in human disease, and the possible downstream effects.

> *Confounding Factors: The manuscript neglects critical confounding variables such as comorbidities, medications, and lifestyle factors, which could influence chromatin structure and gene expression independently of AH.*

This is an interesting suggestion. This dataset only contains 4 AH patients, which we have included basic clinical data in Supplemental Table 1, including Age, HCA1c, Bilirubin, AST, ALT, Creatinine, Albumin, and MELD score. 3/4 of these patients are severe AH while 1 is moderate (AH2). Despite one patient being moderate, all four AH patients had similar correlations with each other, suggesting these disease specific differences we observed are not indicative of severity. More patient samples are needed to determine if genome architecture changes throughout disease progression. We have added this important discussion to the manuscript (page 12, lines 5-14).

> ***Recommendations for the authors:***
>
> ***Reviewer #2 (Recommendations for the authors):***
>
> *The criteria used to determine which pairs of regions exhibit significant differences in contact frequency between alcohol-associated hepatitis (AH) and healthy controls (HC) are not disclosed. It would be beneficial for the authors to provide this information, including details such as the number of pairs tested, the nature of the statistical tests conducted, the method of multiple testing correction applied, as well as the significance thresholds used, and the number of loci-pairs below these thresholds for each chromosome. This information would greatly enhance the reader's understanding of the relevance of the reported findings.*

Thank you for this comment, though we are not sure we totally understand. All of our statistics were performed using multiHiCcompare [2], where we input all 8 datasets (.hic files from Juicer), then measured statistical differences between defined groups (HC vs AH). For our randomization studies, we randomized the group comparisons, so each group contained a mix of HC and AH.

> *Second, a formal statistical definition of what constitutes a hotspot would be valuable for clarity.*

Thank you for this suggestion. Initially, hotspots were defined as just regions of the genome with a high frequency of very significant differential contacts. We have defined a more formal definition of “hotspot” based on similar criteria. A hotspot is defined by both adjusted p value and frequency of locations. First, we filtered all pair-wise chromosomal interactions by a very, very stringent padj < 0.0000001 to focus on only the most changed coordinates (Supplemental Table 4). Then we looked for regions of the genome with a high frequency of these differential locations. Borders for each hotspot were determined more liberally by looking at the full list of differential spots (padj < 0.05). Then we used code to list genes within each interacting region. We have added these important details to the Methods (page 14, lines 11-14).

> *Third, a clear definition of the criteria used to identify different topologically associated domains (if these were indeed defined in the data and/or utilized in the analyses) would also be a helpful addition.*

Thank you for this suggestion, we did not identify TADs or really utilize TADs in any of these analyses.

> *Likewise, several statements throughout the paper lack support from specific analyses, although it should be feasible to implement such analyses (or at least present them if they have already been conducted) to substantiate these claims:*
>
> *If randomizing samples does not result in significant differences between (randomized) cohorts, it would be beneficial to provide insights into the number of loci pairs that exhibit differences in frequency when using both the actual and randomized cohorts.*

Thank you for asking this question, as this is an important point. Using multiHiCcompare, if we compare WT (n=4) to AH (n=4), we get the results in the figures and supplementary data but if we randomize Group 1 (WT, WT, AH, AH) vs Group 2 (WT, WT, AH, AH), we get almost 0 significant changes in contact frequency. To show this more robustly, we performed 5 randomized comparisons and found far fewer changes in contact frequency between groups. This shows that these changes in contact frequency caused by disease are not random, but rather due to our real difference in AH. This point has been added to the Results (page 6, lines 15-17), and Methods (page 14, lines 16-21)

> *If most changes in contact frequency occur locally, it would be useful to visualize the relationship between effect sizes and/or significance levels for the observed differences in frequency in relation to the distance between the involved loci. Additionally, comparing these results to the average baseline contact intensities as a function of distance would be informative. This comparison could help determine whether the distance decay in effect size/significance for the differences between AH and HC is faster or slower than the decay rates for baseline contact frequencies.*

This is a good suggestion. In our initial analysis, we made a number of figures relating chromosome positions, distance between loci, and statistics regarding the differential contact frequency. In the initial submission, we only showed Figure 3, which shows the logFC (log fold change) for the differential contact frequency by chromosomal position on both sides. To address this question, we have added a supplemental figure showing logFC as a function of the distance between two loci (new Supplemental Figure 3)

> *Similarly, the assertion that most changes do not affect the structure of topologically associated domains (TADs) but occur either within or between TADs should be supported by specific testing; otherwise, or else, removed.*

Thank you, yes we have adjusted the language in the Discussion

> *Furthermore, the authors should clarify whether differences in chromatin conformation are more pronounced around immune genes compared to genome-wide expectations. If this is not the case, it would be helpful to quantify the intensity of these differences around the highlighted genes in relation to the rest of the genome. To achieve this, I would suggest the following:*
>
> *Conduct enrichment analyses on the genes located within the most prominent hotspots to determine whether they are significantly enriched in immune genes (and, or, alternatively, in any other functional category).*
>
> *Estimate the average absolute fold change in contact frequency within all topologically associated domains (TADs) identified in the study. This would allow for the identification of immune gene-containing TADs highlighted in Figures 5-8, providing readers with a quantitative understanding of how anomalously different these genomic regions are*

> *with regards to the magnitude of its alterations in AH, compared to the rest of the genome.*
>
> *While some of the selected gene clusters appear to co-localize well with topologically associated domains (e.g., Figures 5A, 8A), others seemingly encompass either multiple TADs (Figure 6) or only portions of them (Figure 7). This should be clarified.*

Thank you, this is a great suggestion. In order to be as unbiased as possible, we took all genes present in the regions with the highest significant changes in genome (Supplemental Table 4) that we used to identify the hotspots. And you are correct, we do in fact see enrichment of genes involved in innate immune signaling. This has been added to Results (page 7, lines 19-25) and Figure 4.

> *Finally, there are several minor issues concerning the figures that could be easily addressed to substantially enhance their readability:*
>
> *Font sizes in most figures should be increased, particularly for some axis labels and tick marks. This issue affects most figures; for instance, in Figure 4, it hinders the reader's ability to interpret the ranges of the data presented.*

Thank you, the figures have been adjusted

> *Figures 5 to 8 (panels A and B) would benefit significantly from a more consistent format. Specifically, the gene cluster boxes should also be included in the right panels, and the gene locations should be displayed on the left in a uniform format across all figures (e.g., formatting Figures 7 and 8 to match the style of Figures 5 and 6).*

Figures 5 and 6 have a similar structure to each other because we were focusing on all of the genes in that chromosomal region. Figures 7 and 8 are different because we are focusing on how the region around a certain hotspot of interest changes.

> *It is also important to note that the genes plotted in Figures 8C and 8D are not the same. Concerning these two panels, it would be valuable to clarify whether the data presented pertains exclusively to monocytes. If so, information regarding the number of cells analyzed and the number of donors from which they were drawn would also be beneficial.*

These figures are generated using scRNA-seq data. They represent all of the genes expressed in that region of the genome, in their chromosomal position. If a gene is not expressed in the scRNA-seq data, then it is not shown. I have debated with myself a lot on how to show gene expression in a region of the genome, but I think this is the clearest way to show this; including the genes that have no expression would make it more confusing. But yes, if you compare HC and AH, you see some differences in the list of genes. We have added more clarity to the figure legend for this figure.

References

(1) Kim, A., Bellar, A., McMullen, M. R., Li, X. & Nagy, L. E. Functionally Diverse Inflammatory Responses in Peripheral and Liver Monocytes in Alcohol-Associated Hepatitis. Hepatol Commun 4, 1459-1476 (2020). *https://doi.org*:10.1002/hep4.1563

(2) Stansfield, J. C., Cresswell, K. G. & Dozmorov, M. G. multiHiCcompare: joint normalization and comparative analysis of complex Hi-C experiments. Bioinformatics 35, 2916-2923 (2019). *https://doi.org*:10.1093/bioinformatics/btz048

https://doi.org/10.7554/eLife.102626.2.sa0